Arshad, Ammar; Lindner, Martin; Lehtonen, Matti

An analysis of photo-voltaic hosting capacity in finnish low voltage distribution networks

Article

An Analysis of Photo-Voltaic Hosting Capacity in Finnish Low Voltage Distribution Networks

Ammar Arshad * [ID]**, Martin Lindner and Matti Lehtonen**

Department of Electrical Engineering and Automation, Aalto University, Maarintie 8, 02150 Espoo, Finland; aalto@mlindner.eu (M.L.); matti.lehtonen@aalto.fi (M.L.)
* Correspondence: ammar.arshad@aalto.fi; Tel.: +358-469-679-949

Abstract: The ascending trend of photo-voltaic (PV) utilization on a domestic scale in Finland, calls for a technical aspects review of low voltage (LV) networks. This work investigates the technical factors that limit the PV hosting capacity, in realistic case networks, designed relative to different geographical areas of Finland. A Monte Carlo method based analysis was performed, in order to quantify the hosting capacity of the formulated networks, with balanced and unbalanced feeds, in PV systems and their limiting constraints were evaluated. Finally, the effectiveness of on-load tap changer (OLTC) in increasing the PV penetration, when employed in the LV system, was investigated.

Keywords: low voltage networks; Monte Carlo analysis; Photo-Voltaic systems; PV hosting capacity

1. Introduction

The Finnish government has taken the initiative to increase renewable energy production, to satisfy half of the national power consumption by 2030 [1]. Photo-Voltaic (PV) systems, one of the main sources of green energy, are inherently distributed and about 70% of their capacity in Europe is integrated into low voltage (LV) networks [2]. Moreover, the feed-in tariff scheme introduced, will further increase PV penetration into the LV distribution system and the primary function of LV networks, i.e., electrical energy distribution, will therefore be reverted.

Reverse power flow is implicit during the high generation periods of PVs. Previously, various impact studies of the distributed generation (DG) on distribution network constraints have been conducted and the common problem, associated with PV hosting capacity enhancement, is voltage rise [3,4]. Unequal distribution of PV on different phases can introduce negative-sequence unbalance [5]. Furthermore, Distribution Network Operators (DNOs) also have to critically review the loading constraints of the network—for instance, transformer loading and cable ampacity—before deciding on PV inclusion.

The PV hosting capacity is defined as the maximum penetration of PV that can be tolerated by the distribution systems without violating the constraints of the network [6]. Hosting capacity identification of a particular distribution system helps utilities to make decisions related to PV inclusion in a timely and reliable manner. Various studies have been performed, utilizing different methods for maximizing PV penetration in distribution systems. The single line network simulation of distribution network was employed in [7], where voltage profile violation was the deciding constraint of PV hosting capacity. This simplification of a three-phase network to a single line gives justifiable results for MV distribution networks but not for LV networks, where unbalanced phase loading and PV connections greatly affect the power quality constraints of the distribution network. In [8], PV penetration maximization was simulated on a 9-bus feeder system, in which the PV were attached at the end of the network. This evaluation disregarded the distributed nature of PV and has limited application. Different scenarios were studied in [9] for PV hosting capacity increment, while observing

the limitations on voltage value and transformer capacity constraints. This case study only considered the extreme cases, i.e., integration of PV systems at the start and end of the feeder. Moreover, hosting capacity studies in the rural distribution networks, which were performed in [10,11], utilized the active and reactive power controls of the network and the enhancement of the voltage band with the on-load tap changer (OLTC). In addition, using the voltage control methods, Walling et al. [2] defined the concept of a critical length of feeder that imposes restrictions on voltage value and cable thermal limits with an increasing PV penetration.

In the papers reviewed, the performance index utilized for the determination of PV hosting capacity was mainly voltage value criteria. In [12,13], thermal limits of conductors were taken to be one of the network constraints, while the transformer capacity was the performance factor considered in [14,15]. Moreover, voltage unbalance was used as a performance constraint in [7,16]. To model the unpredictability of the size and position of the load and PVs, Monte Carlo based studies of PV hosting capacity were performed in [17–20]. In [17], different scenarios, like PV location, voltage regulator existence and power factor of PV inverter, were exploited to thoroughly measure their effects on the hosting capacity. The work was further extended in [18] and the sensitivity of the hosting capacity to the feeder and PV system characteristics were analyzed and optimized control of all the actors in the distribution system was defined, to maximize PV penetration. In [19,20], same multi-scenario based hosting capacity evaluation was conducted for various regions, based on geography (rural and urban).

This study proposes a Monte Carlo (MC) based investigation of PV hosting capacity for various Finnish regional LV networks. Firstly, test networks were developed while considering the different loading profiles of the areas and the compliance of the network with the limiting constraints, like component ampacity and the standard, EN 50160 [21], which allows ±10% voltage deviation from nominal, at the customer connection. For test network simulations, different LV network components were modelled. LV network components included: distribution transformer, cables, load and PV modules. In addition, the backward-forward sweep method that is utilized for load flow analysis to calculate the voltages and currents of nodes and branches, respectively, is briefly explained.

Secondly, the PV hosting capacity of each network was quantified, while adopting different connection schemes for PV, i.e., balanced and single-phase connections. Various limiting constraints were identified that will act as benchmarks for DNOs, while introducing new PV modules in the distribution system and also aid in deciding on countermeasures to increase the hosting capacity of the networks.

Lastly, an on-load tap changer (OLTC) option for MV/LV transformer was utilized and its impact on the increment of hosting capacity was analyzed. A comparative study of the hosting capacity of PV in the LV network for different regions was conducted, with and without, OLTC reinforcement in the secondary substation. The simulated results show that the PV hosting capacity is dependent on the type of connection of PV among phases and the limiting constraints are highly dependent on the region, number of customers and capacity of network components. If a balanced feed-in of the PV is utilized, then there is substantial increase in hosting capacity with the employment of OLTC. However, hosting capacity is not greatly affected in the single-phase connections of PV, as negative sequence voltage unbalance is the limiting constraint in those cases.

2. Modelling and Load Flow

2.1. Load Model and Profiles

In LV systems, usually the loads are resistive in nature, with a small reactive component. Thus, to model resistive load, a high-power factor is assumed and primarily constant power loads are considered, as depicted in the following equation.

$$[S_L{}^{abc}] = [P_{PQ}{}^{abc}] + i[Q_{PQ}{}^{abc}] \tag{1}$$

where $[S_L{}^{abc}]$, $[P_{PQ}{}^{abc}]$ and $[Q_{PQ}{}^{abc}]$ are three element vectors (for phases *a*, *b* and *c*) of total apparent, real and reactive powers of constant power loads.

In order to classify customers into different geographical areas, Eurostat's classification method was utilized, which divides countries into smaller regions based on the Nomenclature of Territorial Units of Statistics (NUTS) [22]. Specifically, it is the NUTS 3 region that under scrutiny, which is classified as follows:

- Predominantly Rural (PR)
- Intermediate (IN)
- Predominantly Urban (PU)

Moreover, load profile is highly dependent on the method of heating in different regions and on the type of customer. For domestic customers, segregation is based upon the type of heating method being utilized in the household. Firstly, the hourly kWh meter readings of houses with varying heating modes were collected and afterwards the survey was conducted on the basis of type of heating system installed. The types of heating method found during data collection were: storage heating (SH), district heating (DH) and direct electric heating (DEH) [23]. For the PR and IN regions, only domestic customers were considered but for the PU region, in addition to domestic load, public and commercial loads were also used in simulations. Public customers were mainly offices and commercial customers were the malls that require energy in bulk amounts.

2.2. Feeder

Carson's line equations were utilized to determine the series impedance of cables [24]. Figure 1a shows a 3-phase 4-wire LV feeder, in which all the phase conductors are considered to be transposed. Firstly, a primitive impedance matrix was formed, as presented in Equation (2). z_{ij}, z_{in}, z_{nj} and z_{nn} are 3×3 matrices. To formulate the 3×3 impedance matrix, the Kron-reduction method was employed. The impedance matrix for a line between two nodes is given by Equation (3) and the detailed explanation is presented in Appendix A. For network formulation of different Finnish regions, only cables were considered for line segments; however, in some rural areas overhead lines are still employed.

$$\left[z_{primitive} \right] = \left[\begin{array}{cc} \lceil z_{ij} \rceil & \lceil z_{in} \rceil \\ \lceil z_{nj} \rceil & \lceil z_{nn} \rceil \end{array} \right] \tag{2}$$

$$z_{mn} = \left[\begin{array}{ccc} z_{aa} & z_{ab} & z_{ac} \\ z_{ba} & z_{bb} & z_{bc} \\ z_{ca} & z_{cb} & z_{cc} \end{array} \right] \tag{3}$$

As the cables were considered to be fully transposed, diagonal elements of the lime impedance matrix were equal to each other and off-diagonal terms were also equal. In addition, $i_{a,b,c}$ are the phase currents of phases *a*, *b* and c respectively. i_n is the neutral wire current and to demonstrate the worst-case scenario zero sequence current, was assumed to be conducted only by the neutral wire and not by earth.

2.3. PV Model

Domestic customers mostly have single-phase-rooftop PVs, while public and commercial customers have three-phase PV systems installed, supported by voltage source inverters (VSI) for integration with the LV network. A negative load model of PV generation [25] and unity power factor operation were considered ($[Q_{PV}{}^{abc}] = 0$), as depicted in Figure 1b. $[S_L^{abc}]$ is a 3-element vector that represents the loads of phases, *a*, *b* and *c*. Furthermore, the inverter efficiency was taken to be 95%.
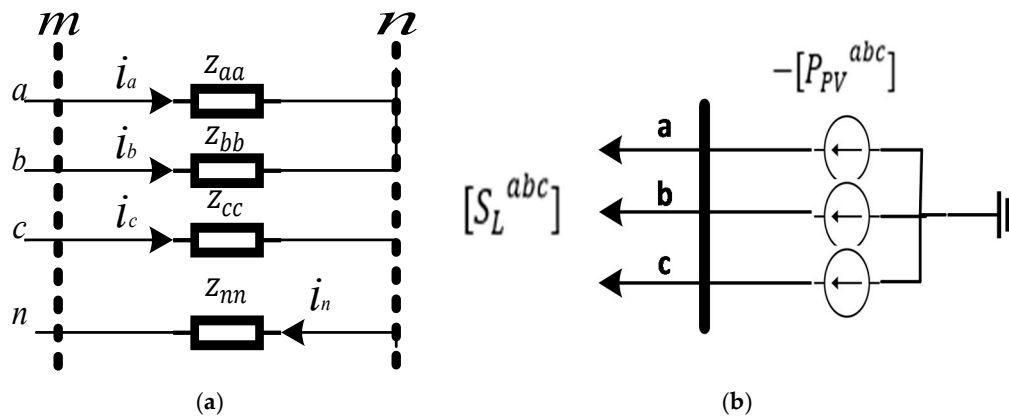
Figure 1. (**a**) Typical representation of a 3-phase 4-wire LV feeder segment; (**b**) Constant negative load PV model.

2.4. Load Flow Analysis

The backward/forward sweep (BFS) method for radial network load flows was applied [26]. Nodes employed in the load flow analysis were: PQ-nodes (load nodes), PU-nodes (PV integrated nodes) and a Slack node (secondary substation transformer). For load flow convergence method, we used an iteration scheme. The steps followed are summarized as:

1. All nodes were initialized with nominal grid voltage.
2. Branch currents were calculated, dependent on the initial voltages.
3. Backward sweep was performed to sum the branch currents, from the end of the feeder to the secondary substation.
4. Forward sweep updated the voltages of the node by calculating the voltage drops until the last node.
5. The algorithm terminated when node voltage change was smaller than a predefined error.

3. Methodology

3.1. Network Constraints

For the formulation of test networks and determination of hosting capacity, critical network constraints were defined. Usually, deciding factors for LV network sizing and topology are node voltage value, ampacity ratings of transformer and cables and negative sequence unbalance. Some specific codes utilized for violated constraints are as follows:

*   Load flow did not converge (E_1)
*   Lower voltage limit violation (E_2)
*   Higher voltage limit violation (E_3)
*   High negative sequence unbalance (E_4)
*   Cable section ampacity violation (E_5)
*   Neutral wire ampacity violation (E_6)
*   Transformer loading violation (E_7)

3.2. Test Network Formation

To devise the test networks for different regions, worst case scenarios were first defined, without considering PV feed-in. Normally, while designing an LV network, voltage drop and peak load demand are the deciding factors for the length of the network. Instead of utilizing yearly data for loading, worst case hours were found by employing a barycenter approach that made use of total

grid load (S_{sum}) and load barycentre ($L_{barycentre}$) along the feeder, as shown in Equations (4) and (5). Load barycenter links the network length with the total network load

$$S_{sum} = \sum_{i=1}^{n_{nodes}} S_i \tag{4}$$

$$L_{barycentre} = \frac{1}{S_{sum}} \cdot \sum_{i=1}^{n_{nodes}} S_i \cdot i \tag{5}$$

where i and S_i are the node number and apparent power of the load attached to it, respectively. The simulation script generates the pairs of the total consumption and its load barycenter along the feeder for each hour, for a particular number of nodes assumed. The (S_{sum}; $L_{barycentre}$) pair gives the measure of network length and its corresponding loading. As the number of nodes are increased, load barycenter values move away from the origin for a particular loading. Thus, the load barycenter gives the impact of the number of nodes on the worst-case scenarios. Loading assumed was based on the regions, as described in Table 1. Distributions of domestic customers were based on various heating modes and the NUTS region classification. Thus, 8760 pairs were generated altogether, for the whole year. The upper right part of the convex hull curve returned points (worst-case hours) for which load flow was conducted. The points selected by the convex hull represented the cases where the network had a large number of nodes and high loading hours. Figure 2 illustrates this idea. The same approach was adopted for the public and commercial customers.

Table 1. Heating mode distributions dependent on different regions.

Regions	Heating Modes		
	Storage Heating (SH) (%)	District Heating (DH) (%)	Direct Electric Heating (DEH) (%)
Predominantly Rural (PR)	5.9	52.9	41.2
Intermediate (IN)	7.6	52.5	39.9
Predominantly Urban (PU)	0.4	95.3	4.2

MC simulations were conducted because of huge number of possible customer permutations, their positions along the feeder and the required calculations for the number of nodes. The uniform probability distribution was utilized for all variables and the large number of iterations were conducted to reduce the probability of yielding wrong results. To determine the maximum size of the network, nodes were incremented sequentially. In addition to geographical locations, the voltage change in the medium voltage (MV) grid is another criterion that affects the sizing and topology of LV networks. Thus, varying voltage changes considered on MV network are 0% and ±5%. The 5% case assumes that there is a 5% voltage rise in the MV network. Hence, considering the standard EN50160, a 5% rise margin is left for the LV network. This is regarded as the base case and is the prevailing situation in the present conventional networks. In the 0% MV voltage change case, a 10% voltage rise due to PV can be allocated to the LV side. Finally, in the −5% case, the voltage control in MV system is assumed to be active, such that an even higher LV network voltage rise is possible. For each specific network size and MV grid voltage change, 5000 sample networks were generated, adopting randomly selected customers and afterwards checking for the constraint violations. The network was considered to be invalid if any one of the constraints was breached for one hour. A 5% network violation tolerance was considered, i.e., 5% of the 5000 MC simulations. A flow diagram of the MC based, adopted approach is presented in Figure 3.
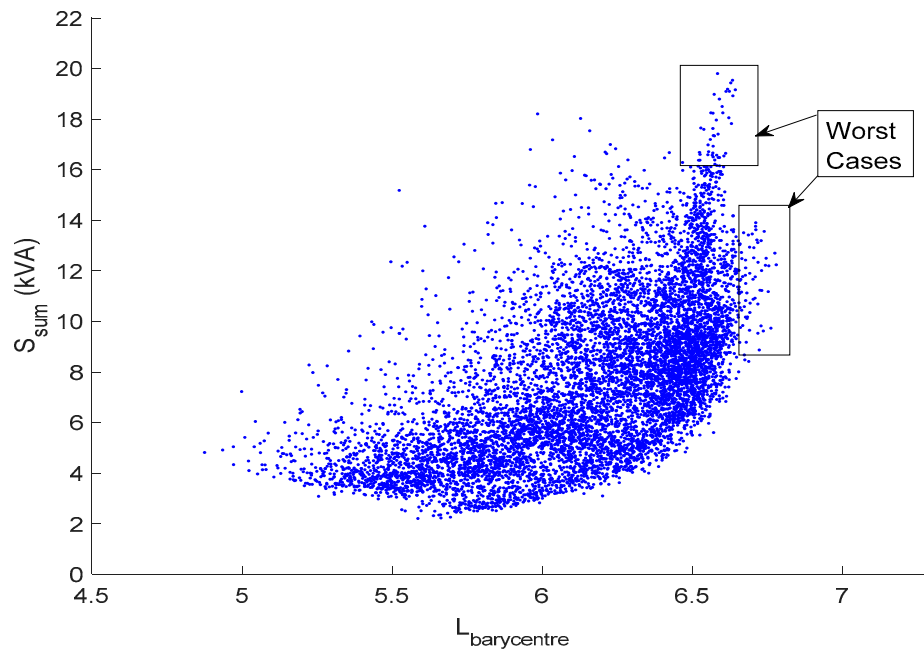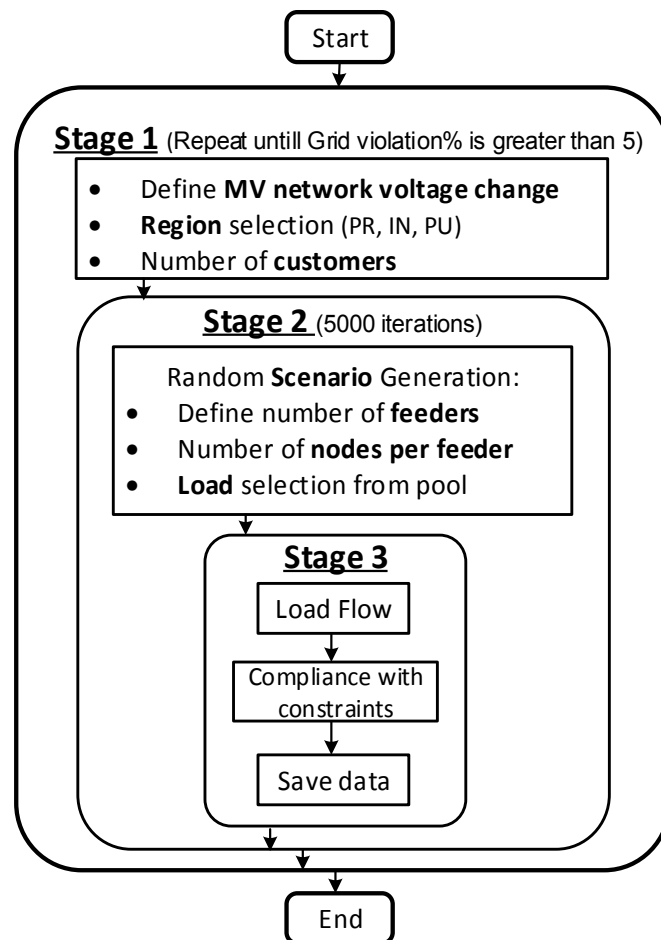
Figure 2. Plot for finding the worst-case hours.

Figure 3. Monte Carlo based algorithm for test network generation, MV represents medium voltage.

3.3. PV Hosting Capacity Determination

Based on the network topologies created in the previous section, the maximum PV hosting capacity was determined. The PV hosting capacity (*HC*) is the ratio of PV peak power to maximum network load. For *HC* calculation, a PV node is made beside the load node. In addition, all the PV nodes are considered to have same real power generation at a particular instant. The worst-case for *HC* simulation has the maximum difference between PV generation and load.

For simulating worst-case hours, data pairs of total LV network load and total PV generation, for 8760 h, were generated and convex hull curve were employed. The dataset of worst-cases, for PV hosting capacity determination, were found to be in the upper left corner, depicting the hours having the maximum PV generation and minimum network load. The barycenter approach was not used, because all PVs have the same generation profile, which give a barycenter in the center of the feeder. Once the worst-case hours were known, same MC approach, as in Figure 3, was implemented, with slight changes in the input parameters for stage 1. The modification was the inclusion of the PV nodes. Furthermore, load flow analysis was also modified to include the impact of the PV nodes. To determine the maximum hosting capacity of the case networks, the power production level of each installed PV module was increased, step by step, up to the maximum generation at that particular hour. The MC simulation algorithm checked the compliance of the generated grids, against the previously defined constraints. If the constraints were not violated, then the PV generation was further incremented. However, when secondary substation was equipped with the OLTC, then the tap position also had to be defined in stage 1.

On the basis of PV inverter connections among phases, two considered orientations were:

1. Balanced PV feed-in
2. Unbalanced PV feed-in (single phase)

In the balanced feed-in, symmetrical distribution of PVs was considered along all the phases for domestic customers. For public and commercial customers, a three-phase connection of the grid tied inverter was used, as the PV systems were quite large. For single phase connections, PVs were connected randomly along the phases. However, balanced customer loading of the phases was employed in both cases.

4. Case Studies and Results

4.1. Test Network Simulations

This section describes how the test networks were created for the analysis. The idea was to model fully-loaded LV networks, the PV hosting capacity of which, is analyzed in Sections 4.2 and 4.3. MC simulations were conducted for all three MV grid voltage changes, for defined geographical regions. The assumed component specifications of the LV grid are depicted in Tables 2 and 3. The assumptions of various LV networks component parameters were based on the Finnish distribution system and the grids were fully loaded, to assume the worst-case scenario for the test network simulations. Formulated test networks, based on the MC simulations and compliance with the constraints, had different topologies, which are described in Tables 4 and 5. The urban domestic networks are pictorially represented in Figure 4.

Table 2. Low Voltage (LV) grid component parameters for domestic customers.

Region	Transformer S_r (kVA)	Cable Length (m)	Customer per Node	Cable
PR	50	150	1	*AXMK* 4×70 mm^2
IN	200	100	4	*AXMK* 4×185 mm^2
PU	1000	100	60	$2 \times AXMK \, 4 \times 185$ mm^2

Table 3. LV grid component parameters for public and commercial customers in urban areas.

| Region	Customer Type	Transformer S_r (kVA)	Cable Length (m)	Customer per Node	Cable
PU	Public	1000	100	2 big customers	$2 \times AXMK\, 4 \times 185$ mm^2
	Commercial	2500		1 big customer	

Table 4. Test network parameters and their limiting constraints for domestic customers.

Region	MV Change	No. of Feeder	Nodes per Feeder	Total Customers	Limiting Constraint
	−5%	1	6	6	E2
PR	0%	1	8	8	E2
	5%	1	10	10	E7,E2
	−5%	3	3,2,2	28	E2
IN	0%	3	4,3,3	40	E2,E7
	5%	3	5,5,4	56	E7,E2
	−5%	3	2,1,1	240	E2
PU	0%	3	2,2,1	300	E5,E7
	5%	3	2,2,1	300	E5,E7

Table 5. Test network parameters and their limiting constraints for public and commercial customers.

Region	Customer Type	MV Change	No. of Feeder	Nodes per Feeder	Total Customers	Limiting Constraint
PU	Public	±5%, 0%	3	1,1,1	6 big cust.	E5
	Commercial	±5%, 0%	2	1,1	2 big cust.	E5

In the PR region, customers were in close vicinity of the MV network, so the transformer size was small and the number of feeder and customers per node was restricted to one each. For −5% and 0% MV change cases, the lower voltage limit was the deciding factor in the network length. However, in the +5% MV rise scenario, the low voltage problem was mitigated, but extra nodes introduced a violated transformer loading capacity. Moreover, the low voltage problem was a secondary issue.
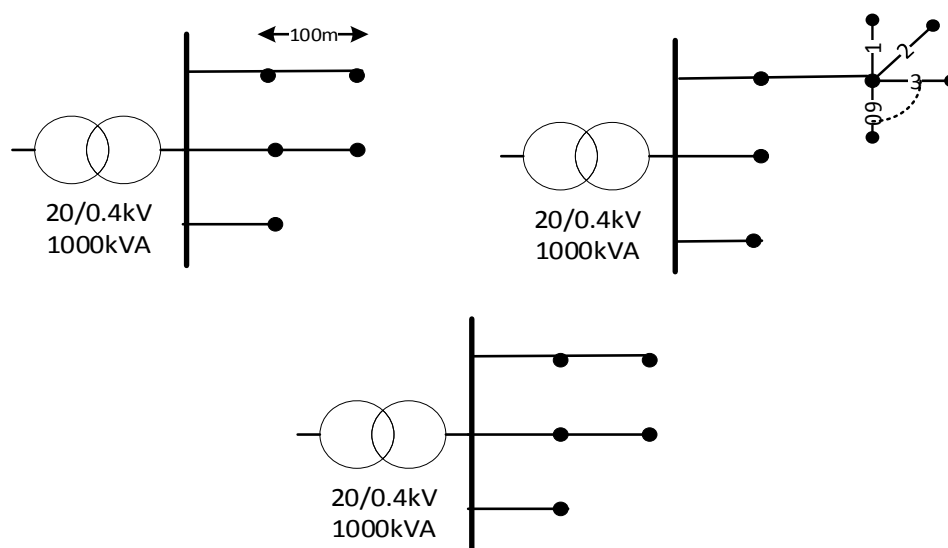
Figure 4. Domestic urban networks for 0% (upper left), −5% (right) and +5% (middle) MV network voltage changes.

In the IN region, four customers could be added to the load node (cable box) of the feeder. To exploit the transformer ampacity, several feeders were added to the network. For −5% and 0% MV changes, the lower voltage band limits of the constructed grids were the deciding factor of network topology, while in the later scenario (nominal MV) transformer loading was the secondary issue to *E2*. *E7* exceeded its nominal rating in the +5% MV rise case.

Lastly, in PU grid formulations, three different customer types were considered. The total number of customers per cable box, for the domestic scenario, were taken to be sixty and two parallel cables utilized. The resultant grids were quite small, due to a high population density. In the case of −5% drop, low voltage was the constraint restricting the grid size. For 0% and +5% MV change cases, the load current exceeding the cable ampacity was the primary limitation and transformer loading was the secondary concern, in case cables are upgraded. In public customer cases, for all the MV change scenarios, cable ampacity was the limiting factor. The grid formulated had a restriction of two nodes per feeder and each node had two big customers (office building) connected to it. In commercial areas, the grid formulation returned a two-feeder grid, with a node each. As in the public customer type simulation, *E5* was the grid-size restricting constraint for the commercial customers. In all urban cases, the transformers were usually in the close proximity of the customer, especially in public and commercial cases.

4.2. Case 1: Network PV Hosting Capacities (Without OLTC)

Based on the type of PV connection in LV networks, two different sets of MC simulations were conducted—one for balanced feed-in (PVs are attached to all the three phases equally) and other for unbalanced feed-in (random single-phase connection). For domestic customers, a 1 kW PV system time series was utilized, while for public and commercial customers in urban areas, 30 kW and 150 kW installed capacities were used, respectively. The mean value of maximal PV hosting capacity, without limit violation in every set of MC simulations of a sample grid, was determined and is presented in Tables 6 and 7.

In the balanced feed-in scenario, the PR region transformer loading was exceeded for the −5% MV drop case. However, for the 0% and +5% MV change cases, the upper voltage limit violation was the primary constraint. In the IN region, the PV hosting capacities in the −5% and 0% MV changes, were predominantly limited by the transformer loading, as there were three feeders originating from the transformer in each case. For the +5% MV rise scenario, over-voltage was the deciding factor for the maximum PV hosting capacity of the network. The PU domestic region's primary limiting constraint was the cable ampacity, due to a large customer density per node. If the network is reinforced; cables are upgraded and the transformer ampacity will be violated. The same trend of cable ampacity violation was prominent in public and commercial customers. In public and commercial customer cases, the customer density was not large, but the power demand by individual customers was quite large, relative to the domestic customers.

Table 6. Test Networks' mean *HCs* and their limiting constraints.

Region	MV Drop	Balanced (3-Phase)		Unbalanced (1-Phase)	
		μ_{HC} (%)	Limiting Constraint	μ_{HC} (%)	Limiting Constraint
PR	−5%	279.2	*E7*	155.9	*E7,E4*
	0%	198.1	*E3,E7*	128.9	*E4,E7*
	5%	117.2	*E3*	87.7	*E3*
IN	−5%	273.9	*E7*	156.3	*E7*
	0%	233.5	*E7*	117.4	*E7*
	5%	154.6	*E3,E7*	98.2	*E3,E7*
PU	−5%	246.4	*E5,E7*	95.9	*E4,E6*
	0%	239.7	*E5,E7*	95.4	*E6,E4*
	5%	242.5	*E5,E7*	86.8	*E3,E6*

Table 7. Test Networks' (public and commercial) mean *HCs* and their limiting constraints.

Region	MV Drop	Public		Commercial	
		μ_{HC} (%)	Limiting Constraint	μ_{HC} (%)	Limiting Constraint
PU	−5%	127.63	*E5*	167.19	*E5*
	0%	125.73	*E5*	165.17	*E5*
	5%	123.7	*E5*	169.63	*E5*

The single phase feed-in of PVs gives rise to the negative sequence unbalance that should be below the 2% level. Moreover, due to single phase connections, the transformer winding's ampacity was also a limitation. The calculated PV hosting capacity in single phase connections was significantly lower than the balanced feed, as depicted by the bar graph in Figure 5. In the PR area, the −5% MV drop case had a transformer capacity limitation, while for 0% voltage, unbalance was an issue; due to single phase PV introduction. The +5% MV case had a predominant limitation of an over-voltage limit violation. For the IN region for all MV values, the same constraints of *E3* and *E7* were violated as in the balanced feed-in scenario. The PU region had the largest reduction in hosting capacity, as compared to its balanced case. Primarily, negative sequence voltage unbalance, which resulted in secondary limit violation of neutral wire ampacity, was the limiting constraint in the −5% MV drop case and vice versa for the nominal MV case. Lastly, in the +5% MV rise case, a large number of PV connections, led to an over-voltage problem.
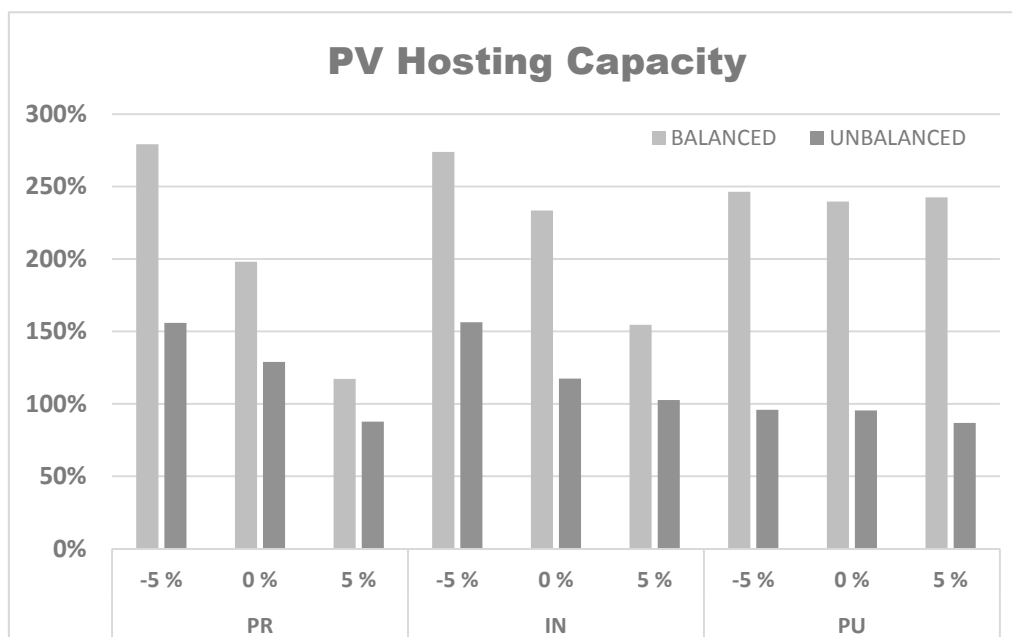
Figure 5. Photo-voltaic (PV) hosting capacity for balanced and unbalanced PV feed-in, for domestic customers.

4.3. Case 2: PV Hosting Capacity (With OLTC)

The case 1 analysis showed that there were six occasions when the high voltage at the nodes was the primary limiting constraint for the LV network hosting capacity. The goal was to maximize the hosting capacity of the specific case networks. To mitigate this issue an active voltage control was applied that lowered the ratio of the secondary substation transformer, in the case of excess voltage at customer nodes. For this purpose, secondary substation, equipped with OLTC and PV hosting capacities, was again evaluated with varying ratios. The results indicated that it is not necessary to

lower the transformer's voltage ratio to −10% to achieve a maximum hosting capacity, as the limiting constraints change with increasing PV penetration into the system. The cases with the voltage rise limitation are:

1. Balanced cases:

   - PR (0% and +5% MV rise)
   - IN (+5% MV rise)

2. Single phase case:

   - PR, IN and PU (+5% MV rise)

For all balanced feed-in cases, the limiting constraint changed from over-voltage (*E3*) to transformer loading (*E7*). In the 0% and +5% MV change cases, the hosting capacity increased by 17.5% and 43.5%, respectively. Meanwhile, for the IN +5% MV change scenario, the hosting capacity increased by 34% of the previous case value.

For the unbalanced cases, in the PR and IN scenarios of +5% MV change, the *HC* limitation was modified to a negative sequence voltage unbalance (*E4*) and the hosting capacities were increased by 12.5% and 4.5%, respectively. However, in the PU region, single phase feed-in scenario, the limiting constraints returned by MC simulations were *E6* and *E4*. Nevertheless, the increment in hosting capacity was by 7.2%, as compared to the balanced feed-in. In all the single phase cases, at lower tap positions, the lower voltage level became the secondary limit, as the lower voltage limit was violated by phases with which the PVs were not attached. Figure 6 presents a comparison of the hosting capacities, before and after, OLTC employment.
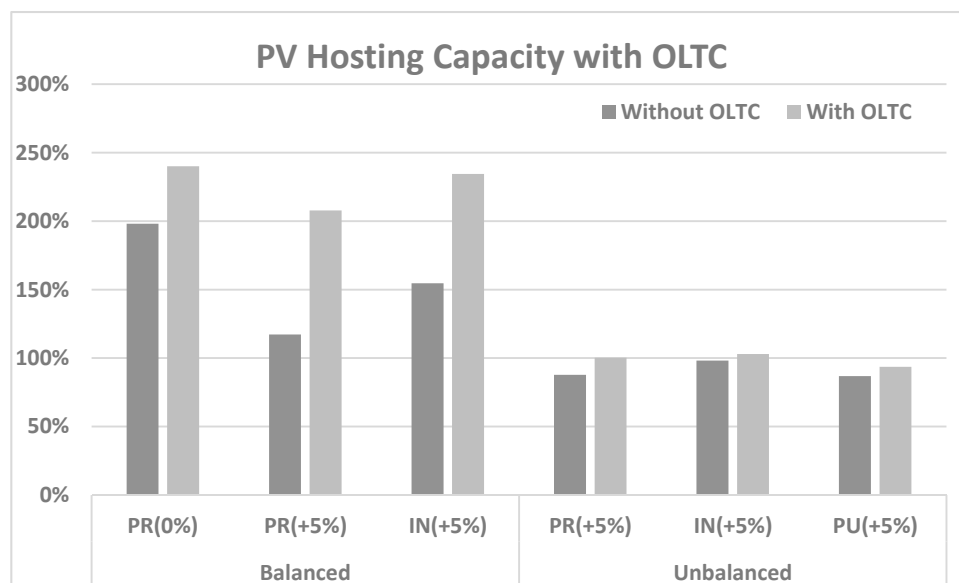

Figure 6. PV hosting capacity, with and without, OLTC inclusion.

5. Discussion

MC simulations were conducted and three different scenarios of MV network voltage changes were considered. However, MV network voltage changes were taken to be constant, which is not the case in reality, because power flow from the adjacent LV networks also affects the MV grid. This a topic for further research.

The number of iterations in MC simulations were also critical to defining the limiting constraints for various scenarios. A low number leads to an inaccurate result, while too many iterations require

excessive computational time and resources. For instance, for the simulations with 1000 iterations, the percentage variance in the results obtained was 0.61%. However, for 5000 and 10,000 iterations, deviations were 0.189% and 0.14%, respectively (results are related to the intermediate region, having 0% MV change, for test network formation simulations). Thus, for the cases in which limiting constraints, for a particular grid, are decided based on very small margins; this slight percentage deviation among various MC simulations is decisive and can lead to the wrong result.

The LV network simulations performed gave limiting constraints for the PV hosting capacity, with and without, OLTC employed at the secondary substation and set a benchmark for constraints in planning a network and decision-making process with PV incorporation. In balanced feed-in scenarios, the hosting capacities in PR and IN regions can be increased by utilizing larger transformers, equipped with OLTC. However, the PU region requires network cable reinforcement, as ampacity is the major issue due to large customer density in domestic regions and larger customer loads in public and commercial regions. The hosting capacity augmentation by OLTC operation is undoubtedly significant. Thus, to enhance PV penetration for balanced feed-in cases, an upgrade to active voltage control is a solution. In single phase feed-in, voltage unbalance and neutral wire ampacity violation are the main issues. The results for the OLTC inclusion showed that the increment in PV hosting capacity of the network was not as significant as in the balanced feed-in case.

6. Conclusions

A Monte Carlo based approach was employed to design and investigate the test networks, based on different Finnish regions. Furthermore, the PV hosting capacities of the designed networks were calculated, with and without, OLTC employment in the secondary substation.

Test network formulations for different regions consequently gave the voltage level violation and transformer loading capacity as the deciding factors in sizing LV networks, for the PR and IN regions. However, the PU region had cable ampacity as the deciding factor, due to its large customer density.

The PV hosting capacities of the formulated LV networks were quantified, with and without, OLTC involvement. For balanced PV feed-in, the hosting capacity was significantly larger and over-voltage was the limiting constraint. However, in the single phase feed-in of PV, it reduced to two thirds of the balanced feed-in capacities for PR and IN regions. Moreover, in the PU regions the hosting capacity was reduced by more than half, as compared to the balanced feed-in. However, negative sequence unbalance and the neutral wire ampacity were the main limiting constraints which define the upper limit of the hosting capacity.

The OLTC reinforcement scenario had significant impacts on the hosting capacity when balanced feed-in was considered. However, for single phase PV installations, the increment was quite minor. DNOs have to carefully integrate PV systems in the LV networks and should take into account the OLTC installation cost, to cope with the higher PV generation, while reinforcing secondary substation. Further research should include a more precise analysis of combined LV and MV network voltage variations.

Author Contributions: All the authors made significant contributions in the paper. Ammar Arshad made theoretical analysis, performed simulations and also wrote the paper. Martin Lindner collected data and performed the preliminary research in his master thesis. Matti Lehtonen supervised the work and commented on paper structure, language and format.

Conflicts of Interest: The authors declare no conflict of interest.

Appendix A

Carson's Equations for Cable Modelling

Figure A1 depicts the concentric neutral cable. The data required to calculate the impedance of the line segment of concentric neutral cable is as follows:

d_c = phase conductor diameter

d_{od} = nominal diameter over the concentric neutrals of the cable

d_s = diameter of a concentric neutral strand

GMR_c = geometric mean radius of the phase conductors

GMR_s = geometric mean radius of the neutral strand

r_c = resistance of the phase conductor

r_s = resistance of a solid neutral strand
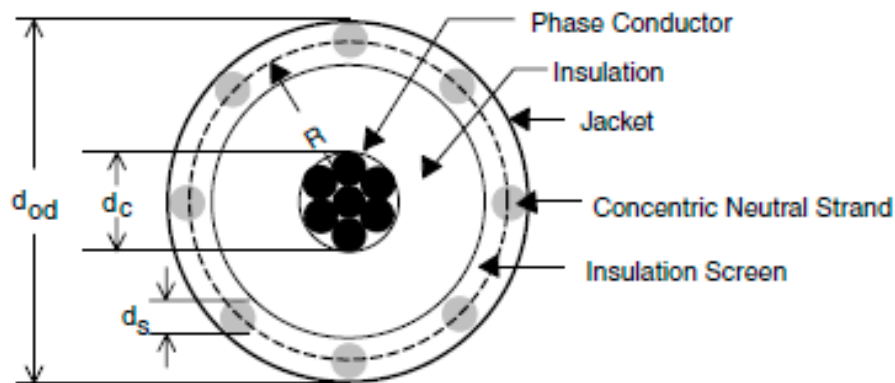
k = number of concentric neutral strands

Figure A1. Concentric neutral cable cross-sectional diagram.

GMRs of the phase conductor and a neutral strand are given in the conductor data cable. To calculate the geometric mean radius of the concentric neutral, the following formula is used:

$$GMR_{cn} = \sqrt[k]{GMR_s \cdot k \cdot R^{k-1}} \qquad (A1)$$

R = radius of a circle passing through the center of the concentric neutral strands

$$R = \frac{d_{od} - d_s}{24} \qquad (A2)$$

The equivalent resistance of the concentric neutral is

$$r_{cn} = \frac{r_s}{k} \qquad (A3)$$

Spacing between the concentric neutral to its own phase conductor is:

$$D_{ij} = R \qquad (A4)$$

Concentric neutral to an adjacent concentric neutral is:

$$D_{ij} = \text{center-to-center distance of the phase conductors.}$$

Concentric neutral to an adjacent phase conductor is calculated by:

$$D_{ij} = \sqrt[k]{D_{nm}^k - R^k} \tag{A5}$$

D_{nm} is the center to center distance between the phase conductors, as shown in Figure A2.
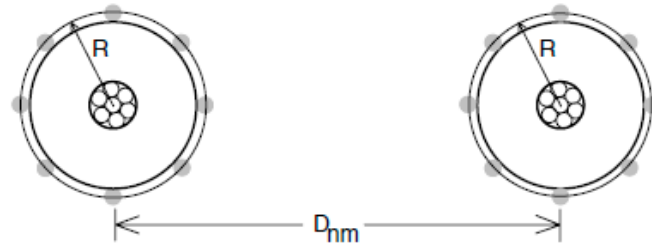

Figure A2. Distance between concentric neutral cables.

The simplified Carson's equations used to obtain the primitive matrix of impedance are:

$$z_{ii} = r_i + 0.09530 + j0.12134 \left(\ln\left(\frac{1}{GMR_i} \right) + 7.93402 \right) \tag{A6}$$

$$z_{ij} = 0.09530 + j0.12134 \left(\ln\left(\frac{1}{D_{ij}} \right) + 7.93402 \right) \tag{A7}$$

and the primitive matrix is:

$$\left[z_{primitive} \right] = \left[\begin{array}{cc} \left\lceil z_{ij} \right\rceil & \left\lceil z_{in} \right\rceil \\ \left\lceil z_{nj} \right\rceil & \left\lceil z_{nn} \right\rceil \end{array} \right]$$

To obtain the impedance matrix for a cable section, the Kron-reduction technique is applied while using the equation:

$$z_{mn} = \left[z_{ij} \right] - \left[z_{in} \right] \cdot \left[z_{nn} \right]^{-1} \cdot \left[z_{nj} \right] \tag{A8}$$

The final impedance matrix obtained is:

$$z_{mn} = \left[\begin{array}{ccc} z_{aa} & z_{ab} & z_{ac} \\ z_{ba} & z_{bb} & z_{bc} \\ z_{ca} & z_{cb} & z_{cc} \end{array} \right]$$

References

1. D&I Alert-Energy. Infrastructure & Natural Recourses Report; New Support Scheme for Renewables in Finland as of 2018. D&I Alert-Energy: 25th November 2016. Available online: http://www.dittmar.fi/sites/default/files/articlefiles/2016_11_25_Alert_Energy.pdf (accessed on 15 August 2017).
2. Walling, R.A.; Saint, R.; Dugan, R.C.; Burke, J.; Kojovic, L.A. Summary of Distributed Resources Impact on Power Delivery Systems. *IEEE Trans. Power Deliv.* **2008**, *23*, 1636–1644. [CrossRef]
3. Navarro, A.; Ochoa, L.F.; Randles, D. Monte Carlo-Based Assessment of PV Impacts on Real UK Low Voltage Networks. In Proceedings of the 2013 IEEE PES General Meeting, Vancouver, BC, Canada, 21–25 July 2013.
4. Shahnia, F.; Majumder, R.; Ghosh, A.; Ledwich, G.; Zare, F. Sensitivity analysis of voltage imbalance in distribution networks with rooftop PVs. In Proceedings of the PES General Meeting, Minneapolis, MN, USA, 25–29 July 2010; IEEE: Piscataway, NJ, USA; pp. 1–8.
5. Seuss, J.; Reno, M.J.; Broderick, R.J.; Grijalva, S. Improving distribution network PV hosting capacity via smart inverter reactive power support. In Proceedings of the 2015 IEEE Power Energy Society General Meeting, Denver, CO, USA, 26–30 July 2015; pp. 1–5.

6. Lin, C.; Hsieh, W.; Chen, C.; Hsu, C.; Ku, T. Optimization of photovoltaic penetration in distribution systems considering annual duration curve of solar irradiation. *IEEE Trans. Power Syst.* **2012**, *27*, 1090–1097. [CrossRef]

7. Kordkheili, R.A.; Bak-Jensen, B.; R-Pillai, J.; Mahat, P. Determining maximum photovoltaic penetration in a distribution grid considering grid operation limits. In Proceedings of the 2014 IEEE PES General Meeting, Washington, DC, USA, 27–31 July 2014; pp. 1–5.

8. Stetz, T.; Marten, F.; Braun, M. Improved Low Voltage Grid-Integration of Photovoltaic Systems in Germany. *IEEE Trans. Sustain. Energy* **2013**, *4*, 534–542. [CrossRef]

9. Bletterie, B.; Gorsek, A.; Uljanic, B.; Blazic, B.; Woyte, A.; Vu Van, T.; Truyens, F.; Jahn, J. Enhancement of the network hosting capacity—Clearing space for/with PV. In Proceedings of the 25th European Photovoltaic Solar Energy Conference and Exhibition, Valencia, Spain, 6–10 September 2010; pp. 4828–4834.

10. Bletterie, B.; Le Baut, J.; Kadam, S.; Bolgaryn, R.; Abart, A. Hosting capacity of LV networks with extended voltage band. In Proceedings of the 2015 International Symposium on Smart Electric Distribution Systems and Technologies (EDST), Vienna, Austria, 8–11 September 2015; pp. 531–536.

11. Capitanescu, F.; Ochoa, L.F.; Margossian, H.; Hatziargyriou, N.D. Assessing the Potential of Network Reconfiguration to Improve Distributed Generation Hosting Capacity in Active Distribution Systems. *IEEE Trans. Power Syst.* **2015**, *30*, 346–356. [CrossRef]

12. Rylander, M.; Smith, J.; Sunderman, W. Streamlined Method for Determining Distribution System Hosting Capacity. In Proceedings of the 2015 IEEE Rural Electric Power Conference, Asheville, NC, USA, 19–21 April 2015; pp. 3–9.

13. Etherden, N.; Bollen, M.H.J. Increasing the hosting capacity of distribution networks by curtailment of renewable energy resources. In Proceedings of the 2011 IEEE Trondheim PowerTech, Trondheim, Norway, 19–23 June 2011; pp. 1–7.

14. Chaudhary, S.K.; Demirok, E.; Teodorescu, R. Distribution system augmented by DC links for increasing the hosting capacity of PV generation. In Proceedings of the 2012 IEEE International Conference on Power Electronics, Drives and Energy Systems (PEDES), Bengaluru, Karnataka, India, 16–19 December 2012; pp. 1–5.

15. Shayani, R.A.; de Oliveira, M.A.G. Photovoltaic Generation Penetration Limits in Radial Distribution Systems. *IEEE Trans. Power Syst.* **2011**, *26*, 1625–1631. [CrossRef]

16. Carvalho, P.M.S.; Correia, P.F.; Ferreira, L.A.F. Distributed Reactive Power Generation Control for Voltage Rise Mitigation in Distribution Networks. *IEEE Trans. Power Syst.* **2008**, *23*, 766–772. [CrossRef]

17. Ding, F.; Mather, B.; Gotseff, P. Technologies to increase PV hosting capacity in distribution feeders. In Proceedings of the 2016 IEEE Power and Energy Society General Meeting (PESGM), Boston, MA, USA, 17–21 July 2016; pp. 1–5.

18. Ding, F.; Mather, B. On Distributed PV Hosting Capacity Estimation, Sensitivity Study, and Improvement. *IEEE Trans. Sustain. Energy* **2017**, *8*, 1010–1020. [CrossRef]

19. Sarmiento, D.A.; Vergara, P.P.; da Silva, L.C.P.; de Almeida, M.C. Increasing the PV hosting capacity with OLTC technology and PV VAr absorption in a MV/LV rural Brazilian distribution system. In Proceedings of the 2016 17th International Conference on Harmonics and Quality of Power (ICHQP), Belo Horizonte, Brazil, 16–19 October 2016; pp. 395–399.

20. Patsalides, M.; Makrides, G.; Stavrou, A.; Efthymiou, V.; Georghiou, G.E. Assessing the photovoltaic (PV) hosting capacity of distribution grids. In Proceedings of the Mediterranean Conference on Power Generation, Transmission, Distribution and Energy Conversion (MedPower 2016), Belgrade, Serbia, 6–9 November 2016; pp. 1–4.

21. Čumpelík, R.; Keri, P. Undefined parameters and two-limit parameters in standard EN 50160 ED. 3. In Proceedings of the 16th International Scientific Conference on Electric Power Engineering (EPE), Kouty nad Desnou, Czech Republic, 20–22 May 2015; pp. 433–436.

22. Eurostat. Urban-Rural Typology-Statistics Explained. Available online: http://ec.europa.eu/eurostat/cache/RCI/#?vis=urbanrural.urb_typology&lang=en (accessed on 25 July 2017).

23. Degefa, M.Z. Energy Efficiency Analysis of Residential Electric End-Users: Based on Statistical Survey and Hourly Metered Data. Master's Thesis, Department of the Electrical Engineering and Automation, Aalto University, Espoo, Finland, 2010.

24. Kersting, W.H. Series impedance of overhead and Underground Lines. In *Book Distribution System Modeling and Analysis*, 2nd ed.; CRC Press: Mexico, 2002; Volume 3, pp. 77–105, ISBN 0-8493-0812-7.
25. Alam, M.J.E.; Muttaqi, K.M.; Sutanto, D. A comprehensive assessment tool for solar PV impacts on low voltage three phase distribution networks. In Proceedings of the 2nd International Conference on the Developments in Renewable Energy Technology (ICDRET 2012), Dhaka, Bangladesh, 5–7 January 2012; pp. 1–5.
26. Demirok, E.; Kjaer, S.B.; Sera, D.; Teodor-escu, R. Three-phase unbalanced load flow tool for distribution networks. In Proceedings of the 2nd International Workshop on Integration of Solar Power Systems Energynautics GmbH, Lisbon, Portugal, 12–13 November 2012.